



Fast lithium ionic conductivity observed in LiI-MoS₂ composite

Zhixiang Liu^a, Yao Zhang^{a,*}, Jipeng Hao^a, Yunfeng Zhu^b, Xinli Guo^a, Liquan Li^b, Gunnar Sly^c, Hui Wang^d

^a School of Materials Science and Engineering, Jiangsu Key Laboratory of Advanced Metallic Materials, Southeast University, Nanjing 211189, China

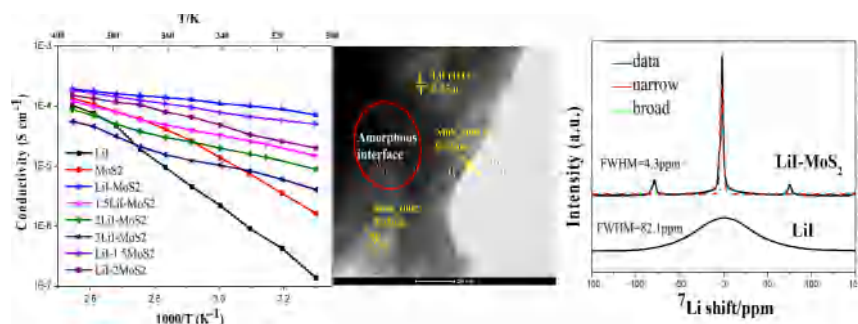
^b College of Materials Science and Engineering, Nanjing Tech University, 5 Xinmofan Road, Nanjing 210009, China

^c Voliland College of Engineering and Architecture (VCEA), Washington State University, Pullman, WA, United States

^d School of Materials Science and Engineering and Guangdong Provincial Key Laboratory of Advanced Energy Storage Materials, South China University of Technology, Guangzhou 510641, China

GRAPHICAL ABSTRACT

The amorphous interface acts as an express way for Li-ion migration.



ARTICLE INFO

Keywords:
Solid electrolyte
LiI
Interface
Ionic mobility

ABSTRACT

The enhancement of lithium ion conductivity is observed in the composite solid electrolyte LiI-MoS₂, which was synthesized by ball milling of the mixture of LiI and MoS₂. The composite electrolyte shows an ionic conductivity as high as $7.1 \times 10^{-5} \text{ S cm}^{-1}$ at room temperature which is nearly three orders of magnitude higher than the pristine LiI and can be ascribed to the formation of the amorphous interface between the two phases. In addition, the composite electrolyte LiI-MoS₂ exhibits a wide apparent electrochemical stability window of -1 to 5 V. X-ray diffraction measurements on the composite inform that original phases are well maintained after ball milling process. Transmission electron microscopy (TEM) and field emission scanning electron microscopy (FE-SEM) reveal the homogeneous distribution of LiI over the surface of MoS₂ and the favorable interface for Li-ion migration between the two phases. Our work proposes a novel strategy to design solid electrolytes with high Li-ion conductive, and also provides some possibility for two-dimensional materials to be applied in superior solid electrolytes.

Huge demands in many energy storage systems have accelerated the development of high-performance rechargeable lithium-ion batteries [1,2]. However, numerous accidents in cell phones and electric vehicles

turn peoples' attention to batteries' safety [3]. Studies have shown that liquid organic electrolytes are liable to cause accidents. They suffer from some serious drawbacks such as lithium dendrite growth,

* Corresponding author.

E-mail address: zhangyao@seu.edu.cn (Y. Zhang).

<https://doi.org/10.1016/j.inoche.2019.107761>

Received 29 October 2019; Received in revised form 26 December 2019; Accepted 30 December 2019

Available online 31 December 2019

1387-7003/ © 2019 Elsevier B.V. All rights reserved.

electrolyte leakage, low chemical stability, flammability and poor compatibility to electrolytes [4,5]. Therefore, alternative high-performance solid electrolytes have drawn considerable attention for replacing organic liquid electrolytes and improving safety of all-solid-state batteries (ASSB) during last decades [6–8]. As far as inorganic solid electrolytes, a few categories with high ionic conductivity have been extensively investigated, including some oxide electrolytes such as perovskite and garnet type materials [9–13] and sulfide electrolytes [14–19]. Both exhibit a high ionic conductivity (10^{-3} – 10^{-4} S cm^{-1}) which approaches to that of commercial liquid organic electrolytes. However, critical drawbacks like low electrochemical decomposition potential, high electrode-electrolyte interfacial resistances and the poor compatibility against lithium of these solid electrolytes hamper their further application in ASSB. LiI has been studied as a solid electrolyte material in the ASSB systems, which is chemically compatible with lithium anodes and has extremely low electronic conductivity. However, the relatively low ionic conductivity (10^{-7} S cm^{-1} at room temperature) of LiI limits its further application [20,21]. In an attempt to increase the ionic conductivity of LiI, Liang and co-workers studied the ionic conductivity of LiI doped with various calcium compounds. The freshly quenched lithium iodide containing 1 mol percent (m/o) of calcium iodide shows a conductivity of 10^{-5} S cm^{-1} at room temperature. However, the conductivity would decrease with time and reach 10^{-6} S cm^{-1} after about 500 hr [22].

Further investigations on the polycrystalline lithium iodide revealed that the conductivity of the lithium iodide based solid electrolyte can be stabilized at 10^{-5} S cm^{-1} at room temperature by the incorporation of Al_2O_3 [23]. However, a dispersion of insoluble dielectric oxide particles such as Al_2O_3 in certain ionic conductors is known to increase total electrical conductivity. Maekawa and co-workers [24] observed a high surface area and pore size controlled mesoporous- Al_2O_3 which lifts the ionic conductivity (2.5×10^{-4} S cm^{-1}) from previously known LiI- Al_2O_3 . The enhancement of the conductivity seems to depend on the pore size, in which smaller pore sizes result in an increase of the conductivity. A formation of the interfacial amorphous phase and its size effect was suggested to be responsible for the enhanced conductivity [25]. Inspired by above work, we paid much attention to the interface which seems more beneficial for Li-ion migration.

In recent years, MoS_2 draws much attention owing to its lamellar structure, large specific area, high chemical stability [26,27] and low electronic conductivity [28]. These made it possible to load solid electrolytes, and likely to be composite electrolytes with high Li-ion migration.

Thus, we synthesized a composite of LiI and 2D material MoS_2 with high Li-ion conductive interfaces by ball milling. A greatly enhanced ionic conductivity (7.1×10^{-5} S cm^{-1} at room temperature) has been achieved in comparison with pristine LiI. Furthermore, the composite electrolyte presents a wide electrochemical window from -1 V to 5 V.

MoS_2 (98%, Aladdin), LiI (99.99%, Alfa Aesar) were used as received. LiI- MoS_2 with different molar ratios of 1:1, 1.5:1, 2:1, 3:1, 1:1.5, 1:2 were synthesized by grinding at a rate of 500 rpm for 10 h under 0.1 MPa argon using a QM-3SP2 planetary mill. The weight ratio of ball to powder was 40:1. In order to avoid the effect of moisture and air to the sample, all operations were operated in a glove box (Etelux lab2000) full of high-purity Ar (purity of 99.9999%, 0.1 MPa, $\text{H}_2\text{O} < 0.1$ ppm and $\text{O}_2 < 0.1$ ppm). The phases of the sample were identified via X-ray diffraction (XRD) measurements on a Rigaku Smart Lab TM 3 kW diffractometer with Cu $\text{K}\alpha$ radiation at a scan rate of 5°min^{-1} . To protect the sample from air and humidity, the samples were covered by an amorphous polymer film (Scotch 810# Magic Tape). Field emission scanning electron microscopy (FE-SEM, Sirion) and Transmission electron microscopy (TEM, FEI Tecnai G2 T20) were used to observe the micro morphologies of the sample. ^7Li Magic Angle Spinning Nuclear Magnetic Resonance (MAS NMR) experiments were conducted to study the Li-ion mobility in the composite. We investigated the electrochemical performances of the composite by

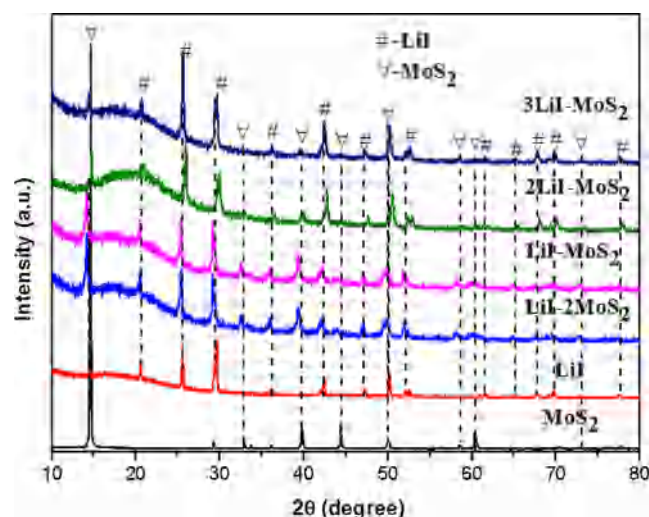


Fig. 1. XRD patterns of LiI- MoS_2 samples after ball milling.

alternating current (AC) impedance spectroscopy, direct-current (DC) polarization cyclic voltammetry (CV) and galvanostatic cycling. The details can be seen in the supporting information.

Phases' structures in the LiI- MoS_2 composite are characterized via X-ray diffraction (XRD). Fig. 1 informs that both phases are well maintained in the composite after ball milling. Any intermediate phases were not detected in the composites, indicating that LiI and MoS_2 have not experienced any interaction or self-decomposition during the ball milling process. The micro-structure of the composite is observed by the transmission electron microscopy (TEM). As shown in Fig. 2(a), well defined layered structures with layered spacing of 0.62 nm of MoS_2 was exhibited, which should be indexed to the (0 0 2) crystal plane of 2H MoS_2 phase. In addition, a lattice fringe of 0.35 nm corresponding to the (1 1 1) crystal plane of LiI phase can be identified as well. It suggests that both LiI and MoS_2 are in perfect crystallinity, which is corresponding to the result of XRD. However, compared to the crystal LiI and MoS_2 phases, the interface between the two phases is identified exactly as an amorphous phase through the analysis of the micro-structure, indicating that LiI is dispersed over the surface of MoS_2 . And the interface is in an amorphous state owing to the high energy ball milling process. Through ball milling, the bulk LiI will cover the specific surface of MoS_2 and forms a large area of amorphous interface which is more beneficial for the mobility of lithium ions [29–32].

The morphology and elemental distribution were further revealed by the application of field emission scanning electron microscopy (FE-SEM) and energy dispersive X-ray spectroscopy (EDS) mapping. The layered structure of MoS_2 can also be detected in the SEM images as shown in Fig. 2(b). In Fig. 2(d–f), we did mapping examination on elements of S, Mo, I, respectively, on the layers. The images suggest that the surface of layered MoS_2 was covered by LiI which was in a homogeneous distribution.

The ionic conductivities of LiI and LiI- MoS_2 with different molar ratios (1:1, 1.5:1, 2:1, 3:1, 1:1.5, 1:2) were measured by electrochemical impedance spectroscopy (EIS) respectively. Nyquist diagrams of LiI- MoS_2 composite samples and the equivalent circuits are shown in Fig. S1. Those semi-circles of Nyquist plots can be well fitted by an equivalent circuit. In the equivalent circuit, components of a resistor R and a capacitance Q are in parallel. The pellet resistance R is defined by the intersection of the semicircle with the Z_{real} axis in the low-frequency limit, which contributes to the conductivity of the electrolyte. As shown in Fig. 3, compared to pristine LiI, LiI- MoS_2 composite samples with different molar ratios (1:1, 1.5:1, 2:1, 3:1, 1:1.5, 1:2) all show higher conductivities than LiI especially at low temperature ranges. When the molar ratio reaches 1:1, the ionic conductivity of the composite attains the highest value of 7.1×10^{-5} S cm^{-1} at room temperature. It is

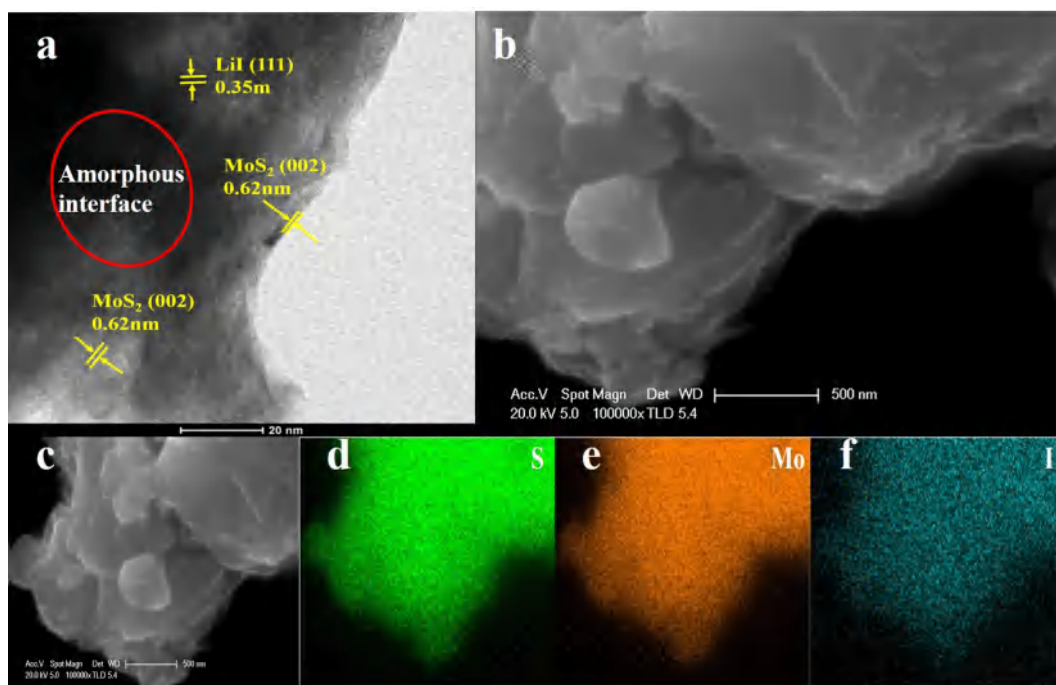


Fig. 2. (a) TEM image of LiI-MoS₂; (b, c) SEM images of LiI-MoS₂; (d-f) EDS elemental mappings of S, Mo, I on the layers, respectively, of (c).

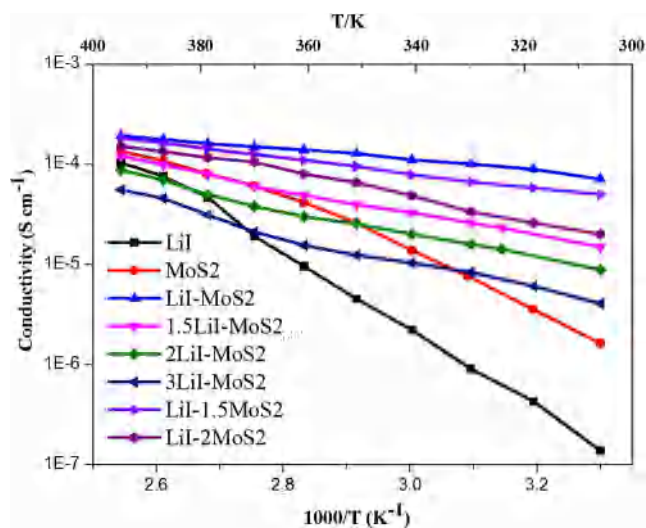


Fig. 3. Temperature dependencies of ionic conductivity for pristine LiI, MoS₂ and different LiI-MoS₂ samples.

nearly three orders of magnitude higher than that of LiI. However when the amount of LiI or MoS₂ increases continuously, its ionic conductivity would decrease to $1.5 \times 10^{-5} \text{ S cm}^{-1}$ for 1.5LiI-MoS₂, $8.8 \times 10^{-6} \text{ S cm}^{-1}$ for 2LiI-MoS₂, $4 \times 10^{-6} \text{ S cm}^{-1}$ for 3LiI-MoS₂, $5 \times 10^{-5} \text{ S cm}^{-1}$ for LiI-1.5MoS₂ and $2 \times 10^{-5} \text{ S cm}^{-1}$ for LiI-2MoS₂, respectively. This phenomenon suggests that excessive LiI or MoS₂ is not helpful for further improving ionic conductivity. They might not form a homogeneous amorphous interface in the composite which is high Li-ion conductive. Excessive LiI or MoS₂ possessing low ionic conductivities may result in the decrease of ionic conductivity. Therefore, 1:1 might be the most proper molar ratio for LiI-MoS₂ composite. The activation energies of LiI and the composite electrolyte LiI-MoS₂ with different molar ratios were calculated (Fig. S2) according to the Arrhenius equation (Eq. (1))

$$\sigma = \sigma_0 \exp\left(-\frac{E_a}{kT}\right) \quad (1)$$

All LiI-MoS₂ composite electrolytes show lower activation energies than that of LiI. The LiI-MoS₂ (1:1) exhibits the lowest activation energy of 0.44 eV, which is a favorable activation energy value for superior ionic conductors ($< 0.5 \text{ eV}$) [33]. The electronic conductivity of the composite was evaluated via the application of DC polarization (as shown in Fig. S3). The electronic conductivity of the composite electrolyte LiI-MoS₂ is $1.3 \times 10^{-8} \text{ S cm}^{-1}$, which is over three orders of magnitude lower than the ionic conductivity of the composite, indicating that the electronic transference is nearly negligible and the migration of Li-ion contributes the majority of the charge transference of the composite electrolyte LiI-MoS₂.

Electrochemical stability of the composite electrolyte LiI-MoS₂ was characterized by cyclic voltammetry of Li|LiI-MoS₂|stainless steel at 5 mV s^{-1} (Fig. 4). For the sample measured in the initial 5 cycles, no additional current emerged in the curve. Only apparent current peaks near 0 V can be observed, which correspond to the Li plating and Li stripping on the stainless steel electrode. It means that the unexpected

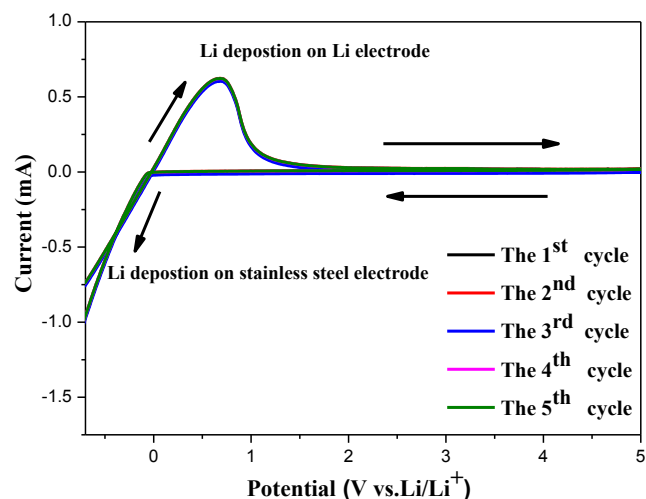


Fig. 4. Cyclic voltammetry curves of LiI-MoS₂ composite. The potential range is from -1 V to 5 V at a scan rate of 5 mV s^{-1} and at a temperature of 303 K .

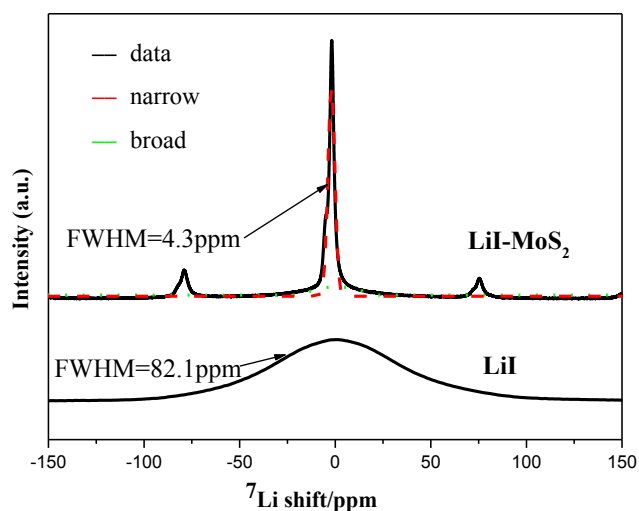


Fig. 5. Solid-state ${}^7\text{Li}$ NMR spectra of LiI-MoS_2 and LiI at room temperature.

electrochemical reaction against the lithium foil should not take place in the sample, which demonstrates the electrochemical stability of the LiI-MoS_2 composite. Galvanostatic cycling curve in Fig. S4 shows long term cycling stability (20 h) without significant voltage fluctuations, suggesting a good electrochemical stability of the LiI-MoS_2 composite against the lithium foil.

Li-ion mobility of the LiI-MoS_2 composite and pristine LiI were evaluated by solid-state nuclear magnetic resonance (Fig. 5). For solid state sample, the transverse relaxation time (T_2), which is inversely proportional to the full width at half maximum (FWHM) of the NMR peaks, is closely related to the ionic mobility of the sample, because high ionic mobility can average the anisotropic dipolar and quadrupolar interactions [34]. Therefore, in this case, the narrow peak is an indication of higher Li-ion mobility. The MAS NMR spectrum of ${}^7\text{Li}$ in LiI exhibits broad peak with a high FWHM value, corresponding to low Li-ion mobility in the bulk LiI . Meanwhile, the spectrum of composite comprises two components, a broad peak and a narrow peak. The overlapping of a broad Gaussian component and a sharp Lorentzian component suggests the co-existence of Li ions with both high mobility and low mobility [35]. In this case, with the utilization of Gaussian Fitting and Lorentzian Fitting on the curve, the spectrum of the composite can be broken down into a broad peak and a narrow peak. The broad peak of the composite is similar to that of pristine LiI , while the narrow one of the composite hints the presence of Li-ions' high mobility, which can be ascribed to the remarkable enhancement in the Li-ion mobility at the interface of LiI and MoS_2 .

In summary, a novel composite solid electrolyte LiI-MoS_2 has been successfully synthesized by ball milling the mixture of LiI and MoS_2 , which shows an ionic conductivity as high as $7.1 \times 10^{-5} \text{ S cm}^{-1}$ at room temperature and a negligible electronic conductivity. From the result of NMR spectra, we can understand that the great enhancement of the ionic conductivity may be assigned to the formation of the highly amorphous interface between the two phases, which acts as a pathway for fast lithium ion conduction. In addition, the composite electrolyte LiI-MoS_2 exhibits a wide apparent electrochemical stability window of -1 to 5 V and demonstrates excellent electrochemical stability against Li foil.

CRedit authorship contribution statement

Zhixiang Liu: Investigation, Data curation, Visualization, Writing - original draft, Formal analysis, Writing - review & editing. **Yao Zhang:** Conceptualization, Methodology, Formal analysis, Software, Resources, Supervision, Writing - review & editing. **Jipeng Hao:** Investigation, Validation, Visualization. **Yunfeng Zhu:** Resources, Writing - review &

editing. **Xinli Guo:** Resources, Validation. **Liquan Li:** Resources. **Gunnar Sly:** Writing - review & editing. **Hui Wang:** Resources, Writing - review & editing, Supervision.

Declaration of Competing Interest

The authors declared that they have no conflicts of interest to this work.

Acknowledgements

We are grateful for Jiangsu Key Laboratory for Advanced Metallic Materials (BM2007204); The Six Talent Peaks Project in Jiangsu Province (2015-XNY-002); The Fundamental Research Funds for the Central Universities (3212008101); Open Fund of the Guangdong Provincial Key Laboratory of Advance Energy Storage Materials (AESM201701).

Appendix A. Supplementary material

Supplementary data to this article can be found online at <https://doi.org/10.1016/j.inoche.2019.107761>.

References

- [1] M. Armand, J.M. Tarascon, Building better batteries, *Nature* 451 (2008) 652–657.
- [2] J. Ju, Y. Wang, B. Chen, J. Ma, S. Dong, J. Chai, H. Qu, L. Cui, X. Wu, G. Cui, Integrated interface strategy toward room temperature solid-state lithium batteries, *ACS Appl. Mater. Interfaces* 10 (2018) 13588–13597.
- [3] J. Wen, Y. Yu, C. Chen, A review on lithium-ion batteries safety issues: existing problems and possible solutions, *Mater. Express* 2 (2012) 197–212.
- [4] Y. Wang, W. Zhong, Development of electrolytes towards achieving safe and high-performance energy-storage devices: a review, *Chem. Electro. Chem.* 2 (2015) 22–36.
- [5] Z. Chen, R. Wu, H. Wang, Y. Jiang, L. Jin, Y. Guo, Y. Song, F. Fang, D. Sun, Construction of hybrid hollow architectures by in-situ rooting ultrafine ZnS nanorods within porous carbon polyhedra for enhanced lithium storage properties, *Chem. Eng. J.* 326 (2017) 680–690.
- [6] L. Fan, S. Wei, S. Li, Q. Li, Y. Lu, Recent progress of the solid-state electrolytes for high-energy metal-based batteries, *Adv. Energy Mater.* 8 (2018).
- [7] Z. Zhang, Y. Shao, B. Lotsch, Y. Hu, H. Li, J. Janek, L.F. Nazar, C. Nan, J. Maier, M. Armand, L. Chen, New horizons for inorganic solid state ion conductors, *Energy Environ. Sci.* 11 (2018) 1945–1976.
- [8] X. Han, Y. Gong, K.K. Fu, X. He, G.T. Hitz, J. Dai, A. Pearce, B. Liu, H. Wang, G. Rublo, Y. Mo, V. Thangadurai, E.D. Wachsman, L. Hu, Negating interfacial impedance in garnet-based solid-state Li metal batteries, *Nat. Mater.* 16 (2017) 572–579.
- [9] Y. Inaguma, L.Q. Chen, M. Itho, T. Nakamura, T. Uchida, H. Ikuta, M. Wakihara, High ionic-conductivity in lithium lanthanum titanate, *Solid State Commun.* 86 (1993) 689–693.
- [10] V. Thangadurai, S. Narayanan, D. Pinzaru, Garnet-type solid-state fast Li ion conductors for Li batteries: critical review, *Chem. Soc. Rev.* 43 (2014) 4714–4727.
- [11] R. Pfenninger, S. Afyon, I. Garbayo, M. Struzik, J.L.M. Rupp, Lithium titanate anode thin films for Li-ion solid state battery based on garnets, *Adv. Funct. Mater.* 28 (2018).
- [12] M. Dixit, M. Regala, F. Shen, X. Xiao, K. Hatzell, Tortuosity effects in garnet-type $\text{Li}_7\text{La}_3\text{Zr}_2\text{O}_{12}$ solid electrolytes, *ACS Appl. Mater. Interfaces* 11 (2019) 2022–2030.
- [13] L. Chen, Y. Li, S. Li, L. Fan, C. Nan, J.B. Goodenough, PEO/garnet composite electrolytes for solid-state lithium batteries: from “ceramic-in-polymer” to “polymer-in-ceramic”, *Nano Energy* 46 (2018) 176–184.
- [14] F. Mizuno, A. Hayashi, K. Tadanaga, M. Tatsumisago, New, highly ion-conductive crystals precipitated from $\text{Li}_2\text{S-P}_2\text{S}_5$ glasses, *Adv. Mater.* 17 (2005) 918–921.
- [15] Y. Kato, S. Hori, T. Saito, K. Suzuki, M. Hirayama, A. Mitsui, M. Yonemura, H. Iba, R. Kanno, High-power all-solid-state batteries using sulfide superionic conductors, *Nat. Energy* 1 (2016).
- [16] N. Kamaya, K. Homma, Y. Yamakawa, M. Hirayama, R. Kanno, M. Yonemura, T. Kamiyama, Y. Kato, S. Hama, K. Kawamoto, A lithium superionic conductor, *Nat. Mater.* 10 (2011) 682.
- [17] J. Lau, R.H. DeBlock, D.M. Butts, D.S. Ashby, C.S. Choi, B.S. Dunn, Sulfide solid electrolytes for lithium battery applications, *Adv. Energy Mater.* 8 (2018) 1800933.
- [18] B. Fan, H. Fu, H. Li, B. Xue, X. Zhang, Z. Luo, H. Ma, Ionic conductive $\text{GeS}_2\text{-Ga}_2\text{S}_3\text{-Li}_2\text{S-LiI}$ glass powders prepared by mechanical synthesis, *J. Alloy Compd.* 740 (2018) 61–67.
- [19] M.A.T. Marple, B.G. Aitken, S. Kim, S. Sen, Fast Li-ion dynamics in stoichiometric $\text{Li}_2\text{S-Ga}_2\text{Se}_3\text{-GeSe}_2$ glasses, *Chem. Mater.* 29 (2017) 8704–8710.
- [20] B. Scrosati, Recent advances in lithium solid state batteries, *J. Appl. Electrochem.* 2 (1972) 231–238.
- [21] C.C. Liang, P. Bro, A high-voltage, solid-state battery system. I. Design

- considerations, *J. Electrochem. Soc.* 116 (1969) 1322–2000.
- [22] C.R. Schlaikjer, C.C. Liang, Ionic conduction in calcium doped polycrystalline lithium iodide, *J. Electrochem. Soc.* 118 (1971) 1447–1450.
- [23] C. Liang, Conduction characteristics of lithium iodide aluminum oxide solid electrolytes, *J. Electrochem. Soc.* 120 (1973) 1289–1292.
- [24] H. Maekawa, R. Tanaka, T. Sato, Y. Fujimaki, T. Yamamura, Size-dependent ionic conductivity observed for ordered mesoporous alumina-LiI composite, *Solid State Ionics* 175 (2004) 281–285.
- [25] H. Maekawa, Y. Fujimaki, H. Shen, J. Kawamura, T. Yamamura, Mesopore size dependence of the ionic diffusivity in alumina based composite lithium ionic conductors, *Solid State Ionics* 177 (2006) 2711–2714.
- [26] H. Sun, X. Ji, Y. Qiu, Y. Zhang, Z. Ma, G. Gao, P. Hu, Poor crystalline MoS₂ with highly exposed active sites for the improved hydrogen evolution reaction performance, *J. Alloy Compd.* 777 (2019) 514–523.
- [27] Q.H. Wang, K. Kalantar-Zadeh, A. Kis, J.N. Coleman, M.S. Strano, Electronics and optoelectronics of two-dimensional transition metal dichalcogenides, *Nat. Nanotechnol.* 7 (2012) 699–712.
- [28] A. Splendiani, L. Sun, Y. Zhang, T. Li, J. Kim, C. Chim, G. Galli, F. Wang, Emerging photoluminescence in monolayer MoS₂, *Nano Lett.* 10 (2010) 1271–1275.
- [29] Y.S. Choi, Y. Lee, K.H. Oh, Y.W. Cho, Interface-enhanced Li ion conduction in a LiBH₄-SiO₂ solid electrolyte, *PCCP* 18 (2016) 22540–22547.
- [30] A. Bunde, W. Dieterich, E. Roman, Dispersed ionic conductors and percolation theory, *Phys. Rev. Lett.* 55 (1985) 5.
- [31] T. Springer, R.E. Lechner, *Diffusion in Condensed Matter*, Springer, New York, 2005.
- [32] C.C. Liang, Conduction characteristics of the lithium iodide-aluminum oxide solid electrolytes, *J. Electrochem. Soc.* 120 (1973) 1289–1292.
- [33] X. He, Y. Zhu, Y. Mo, Origin of fast ion diffusion in super-ionic conductors, *Nat. Commun.* 8 (2017) 15893.
- [34] M.J. Duer, *Solid State NMR Spectroscopy*, Blackwell Science Ltd., London, 10 (2002) 9780470999394.
- [35] Y. Xia, N. Machida, X. Wu, C. Lakeman, L. van Wüllen, F. Lange, C. Levi, H. Eckert, S. Anderson, ⁷Li and ⁶Li solid-state NMR studies of structure and dynamics in LiNbO₃-WO₃ solid solutions, *J. Phys. Chem. B* 101 (1997) 9180–9187.